CONTROL SYSTEM WITH SENSORY INTERFACE FOR A NEURAL FOREARM PROSTHESIS

Sorin LAZARESCU[1], Florin ISTUDOR[2], Delia Alexandra PRISECARU[3,*]

This article presents a bidirectional interfacing system for a neural forearm prosthesis that performs two functions: (1) controlling the prosthesis motors with neural signals collected from the nerves in the patient's stump and (2) transmitting signals from the sensors on the prosthesis to the module implanted in the patient's stump to stimulate the patient's nerves and generate tactile sensations to the patient. The interfacing system was created and tested by the authors of this article in the European project NerveRepack.

Keywords: sensory interface; control system; forearm prosthesis.

1. Introduction

Globally, the number of amputations has drastically increased, for both the upper limbs and lower limbs. The cause of an amputation can be classified into traumatic, produced after a physical accident, and non-traumatic, usually as complications of chronic diseases. According to a study published in 2023, the global incidence of traumatic amputations has grown, over the course of 30 years, from 11.37 million to 13.23 million and the global number of amputations followed this growth pattern, increasing from 370.25 million to 552.45 million [1]. In the contemporary context, modern warfare is one of the leading causes of traumatic amputations, as a results of advanced weaponry and preference for explosive devices.

In the current day and age, the most advanced prostheses are myoelectric ones, which use electromyographic signals (EMG) as command signals and thus give the user a more responsive method of control. However, the commercially available prostheses, though technologically advanced, do not contain a method of reproducing tactile sensations. After prolonged use, the users can develop basic tactile sensation, by the indirect tactile response of the residual member to the

[1] PhD student, Dept. of Medicine, University of Medicine and Pharmacy "Carol Davila" Bucharest, Romania, e-mail: sorin.lazarescu@drd.umfcd.ro
[2] Eng., Dept. of Electronics and Telecommunications, National University of Science and Technology POLITEHNICA Bucharest, Romania, e-mail: florin.istudor@drd.upb.ro
[3] * Lector, Dept. of Machine Elements and Tribology, National University of Science and Technology POLITEHNICA Bucharest, Romania, *corresponding author: e-mail: delia.prisecaru@upb.ro

prosthesis movement. Alternatively, there are systems which generate mechanical force in the residual member (like vibrations), proportional to the strength of the tactile sensation [2]. However, researchers are still developing prototypes which can simulate natural tactile sensation [3], like forceful muscle contraction in the residual member [4] and exciting the sensorial nervous fibers, through subdermal neural interfaces [3].

Myoelectric prostheses are controlled through the EMG signals extracted from the patients' residual muscle. When contracting a certain group of muscles, preferably from the residual limb, EMG signals can be recorded and transmitted to the control block as voltage levels. Even though the signals are extracted through muscles, contraction is the result of stimulation through the neural motor path. Practically, EMG sensors are an indirect method of connecting the user's nervous system with the prosthesis, through the muscles, thus permitting the user to control the prosthesis with muscle contractions.

External myoelectric sensors are the most used, as they offer a completely non-invasive method of extracting EMG signals. In most myoelectric prostheses, external sensors are preferred as they are easy to mount and maintain. These sensors are usually placed on the residual member, on muscle groups that still function correctly. There is no medical intervention needed, as they are easily placed and usually masked by prosthesis. Although external myoelectric sensors are a simple and safe way of extracting EMG signals, there are a number of limitations the user has to consider:

•Sensor mounting area management: the placement area must be constantly and consistently cleaned, to avoid dermatologic problems (inflammation, irritation or even infection) and to provide a good enough connection between the muscles and the sensors;

•Small signal to noise ratio: human skin is a great electrical isolator and greatly dampens the usable EMG signals;

•Adherence problems: the skin is not the most adherent material and usual movements combined with the inevitable perspiration may cause sensor movement or even detachment. Because of this, most external myoelectric sensors require daily calibration;

•Unintuitive control method: a certain movement of the prosthesis will be associated with the contraction of a completely physiologically unassociated muscle group. Because of this, patients have to undergo training and exercises in order to learn how to use the prosthesis. This need to "relearn" o new method of controlling your hand, alongside the difficulty it brings, produce prosthesis abandonment in approximately 23% of users [5].

By comparison with myoelectric prostheses, who not only usually offer few functions but are hard to use, neural prostheses use signals acquired from motor fascicles in the patient's residual limb, which are then used as control signals for

the prosthesis. Thus, neural prostheses cut the intermediary muscle layer, which required limb integrity in the sensor mounting zones and had low signal to noise ratio. Furthermore, eliminating muscle contractions provides a much more intuitive control method, as the prosthesis is directly controlled through the peripheral nervous system, similar to a healthy hand.

2. Neural prosthesis command system

The command system proposed in this article was designed and implemented for a neural prosthesis connected with the patient's nervous system through a bidirectional neural interface. The aforementioned interface is implanted in the patient's stump and is connected to both the ulnar and median nerves of the peripheral nervous system. The interface is detailed in [6] and wirelessly transmits the neural motor signals, from the residual limb to the control system, and the sensorial signals from the control system to the sensorial nerve fascicles. The neural interface is equipped with plug electrodes, which present two needle types [6]:

- Motor needles: implanted through surgery to acquire motor signals from the motor fascicles of the median and ulnar nerves. These signals will be sent via WIFI to the command block, will be processed and will be used to control the prosthesis;
- Sensorial needles: also implanted through surgery in the patient's sensorial fascicles of the median and ulnar nerves. These needles are used to stimulate the sensorial nerves of the patient according to the signals acquired from the tactile sensors, mounted on the prosthesis. Thus, it can generate real tactile feeling when the patient touches different objects with the prosthesis.

The block diagram of the proposed system can be observed in Fig. 1.

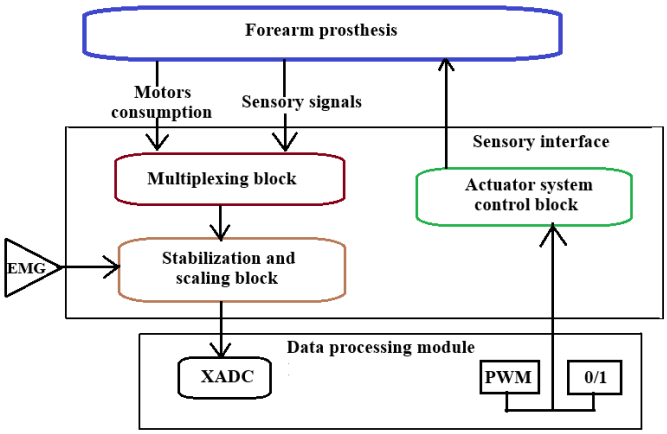

Fig. 1. Block diagram of the control system with sensory interface

The control system contains the following functional blocks:

- The sampling module: converts the analogue signals received from the sensorial interfaces to digital signals, usable by the data processing module;
- Data processing module: applies implemented algorithms to prepare the sampled data for further use;
- Calibration module: allows the user to add coefficients to each individual sampling channel. All the coefficients are additive;
- Movement controller: generates the digital signals required by the drivers in order to produce the movement of the prosthesis;
- Sensorial interface: includes all the external electrical components needed for prosthesis control and for efficient analogue signal transmission, with minimal losses, to the data processing module;
- Control signal generator: generates the external signals used for the prosthesis control. In this paper, as a demonstrator, we have used EMG sensors for controlling the prosthesis;
- VCC (Voltage source): provides the voltage levels and the necessary currents to all the components of the sensorial interface;
- Tactile sensors: each prosthesis finger has a tactile sensor mounted that produces analogue sensorial signals;
- Actuation system: made out of all the motors mounted on the prosthesis;

The data processing module was implemented on an ARTIX-7 AMD Xilinx FPGA platform: XC7A35T-1CPG236C [7], on the Basys 3 development board. The FPGA contains 33280 logic cells (grouped into 5200 configurable logic blocks), 90 digital signals processors, 1800Kb of RAM and an integrated analogue to digital converter (XADC) [7].

For motor control, we have used five CC motor drivers, DRV8838, from Polulu.

The sensorial interface was designed in THT (Through-Hole Technology) and the printed circuit board was fabricated with the help of JLCPCB [11].

The analogue to digital converter integrated in the FPGA provides great space efficiency, but at a relatively high cost. Firstly, the XADC on the Basys 3 board has only four channels connected to external headers, so the sensorial interface contains a channel switching system, using two DG408DJ analogue switches. Thus, the circuit allows the FPGA to sample data from twelve different channels: two independent channels, connected to the external control signals (EMG) and ten other channels, separated in groups of five, connected to the other two header pins available for the XADC header. The sensorial interface has two primary functions: to transmit, scale and filter all analogue data to the XADC and to transmit all digital command data, generated by the FPGA, to the analogue switches and the motor drivers. Both the sensorial interface and the voltage source can be seen in Fig. 2.

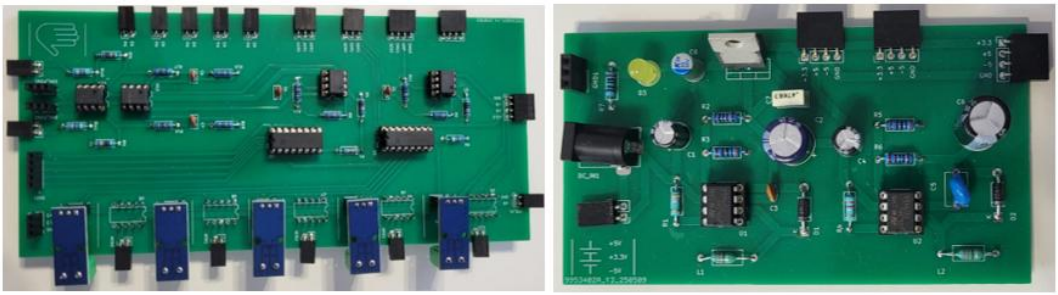

Fig. 2. Sensorial interface (left) and voltage source (right)

All the logic has been implemented in Verilog and SystemVerilog. In total, the project contains 25 modules (9 in Verilog and 16 in SystemVerilog). All the modules used for the system can be seen in Fig. 3.

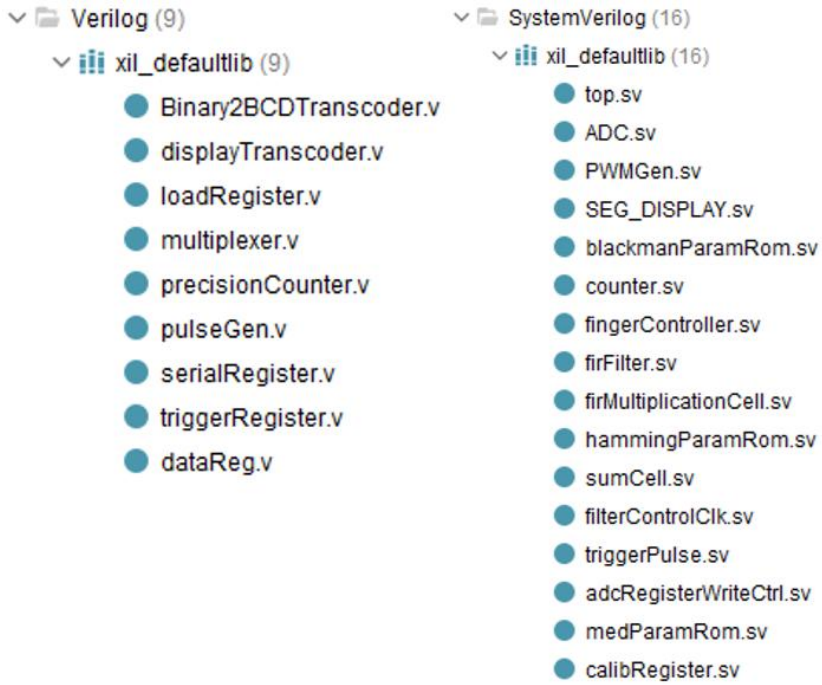

Fig. 3. All Verilog/SystemVerilog files created for the proposed system

As in any electrical circuit, there is unavoidable noise present. Thus, we have implemented a digital filter on the FPGA, using the integrated DSPs, to attenuate the noise. To determinate the best filter parameters, we have analyzed a series of random signals that we have filtered with different digital filters.

To make this analysis, we have used Matlab, as it is optimized for bulk calculus.

For this analysis, we have considered both IIR and FIR filters, with varying parameters, depending on the filter type. All the adjustable parameters can be observed in the table below.

Table 1

Filter parameters

Parameter		Symbol	Values
1	Maximum sampling frequency	Fs_max	160.0256 [kHz]
2	Decimation factor	M	1, 2, 4, 8, 16, 64, 128
3	Sampling frequency	Fs	$Fs = \frac{\mathrm{Fs_{max}}}{\mathrm{M}[kHz]}$
4	Main component frequency	emg_F	150 [Hz]
		senz_F	880 [Hz]
5	Maximum component frequency	emg_Fmax	500 [Hz]
		senz_Fmax	1500 [Hz]
6	Noise maximum frequency	noise_Fmax	$noise_{Fmax} = \frac{\mathrm{Fs_{max}}}{2}[kHz]$
7	Stopband	stopWidth	0.05, 0.1, 0.15, 0.2, 0.25, 0.3, 0.35, 0.4, 0.45, 0.5, 0.55, 0.6, 0.65
8	Maximum passband ripple (IIR)	Rp	0.5, 1, 1.5, 3 [Db]
9	Minimum stopband ripple (IIR)	Rs	30, 40, 50, 60 [Db]
10	Passband normalized frequency (IIR)	Wp	$\mathrm{Wp} = \frac{\mathrm{emg\_Fmax}}{\mathrm{Fs}}$
			$\mathrm{Wp} = \frac{\mathrm{senz\_Fmax}}{\mathrm{Fs}}$
11	Stopband normalized frequency (IIR)	Ws	$Ws = (1 + stopWidth) * Wp$
12	Window type (FIR)	window	Blackman, Kaiser, Hamming
13	Normalized frequency	Wn	$\mathrm{Wn} = \mathrm{Wp} \cup \mathrm{Ws}$
14	Normalized maximum passband ripple (FIR)	dp	0.01, 0.05, 0.1
15	Normalized minimum stopband ripple (FIR)	ds	0.005, 0.01, 0.05

Using the values in Table 1, we have analyzed the randomly generated signals. The resulting parameters can be seen in Table 2.

Table 2

Random signal parameters

Parameters	Symbol	Value
Maximum amplitude (with noise)	$\mathrm{A}_{\mathrm{max}}^{\mathrm{zg}}$	3.33
Minimum amplitude (with noise)	$\mathrm{A}_{\mathrm{min}}^{\mathrm{zg}}$	-3.33
Maximum amplitude (no noise)	$\mathrm{A}_{\mathrm{max}}^{\mathrm{ideal}}$	3.17
Minimum amplitude (no noise)	$\mathrm{A}_{\mathrm{min}}^{\mathrm{ideal}}$	-3.17
Noisy signals mean	E_{zg}	8.97e-4

Ideal signals mean	E_{ideal}	8.55e-4
EMG components	N_{EMG}	10.93
Noise components	N_{ZG}	17.07

Resulting in the following signal to noise ratio (SNR)

$$SNR_{sgn} = 20 \cdot \log_{10}\left(\frac{A_{max}^{ideal}}{A_{max}^{zg} - A_{max}^{ideal}}\right) = 25.939dB \quad (1)$$

Having a SNR of over 20dB, the signals are considered mildly noisy.

The randomly generated signals have been filtered with filters created based on the parameters in table 1. For each filter, we have applied a total of 10000 randomly generated test signals and have extracted the best filter parameters for each tested filter type. The best filters are finite impulse response filters, which is a hopeful result, as it is much easier to implement FIR filters on an FPGA than it is IIR filters.

3. Tests and results

The performance of the sensorial interface was tested in a real environment using the prosthetic hand from NerveRepack project (Fig. 4).

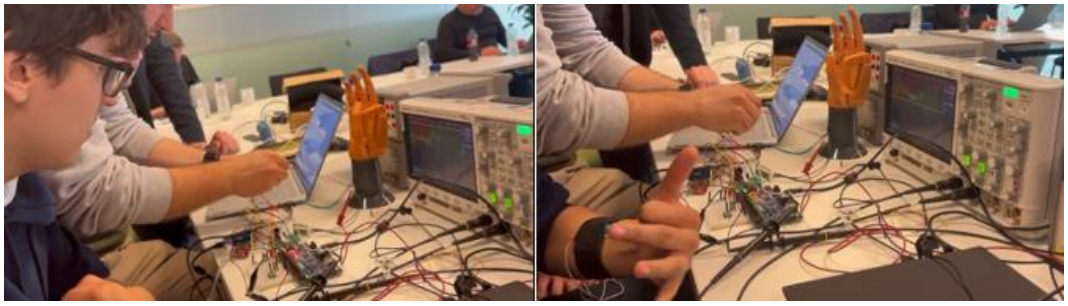

Fig. 4. Testing the interface on the prosthesis from NerveRepack project

Firstly, the XADC user guide suggests introducing a delay between samples, in order to stabilize the voltage level on the sampling capacitor. For the first test, we have used constant values to analyze the static noise of the interface. In table 3, we have introduced the constant values used for testing.

Table 3

Channel values used for testing

Channel	EMG0	EMG1	AMP0	AMP1	AMP2	AMP3	AMP4	SENZ0	SENZ1	SENZ2	SENZ3	SENZ4	TMP	VCC
Value [V]	0	1	0.5	0.5	0.5	0.5	0.5	0	0	0	1	0	-	-

The first parameter we have analyzed is the maximum voltage amplitude between consecutive samples. Ideally, this value should be 0, as we are providing constant values through all the channels. We have analyzed the impact of the sampling delay (tdelay) on the mentioned parameter. The results can be seen in Fig. 4. It is apparent that increasing the delay causes the inter-sample noise to decrease, but it also causes the sampling frequency to decrease. In order to keep the best out of both, we have chosen to continue testing with tdelay = 700 clock cycles (7µs), which presents a mean inter-sample noise of just under 25mV (2.5% of the maximum value).

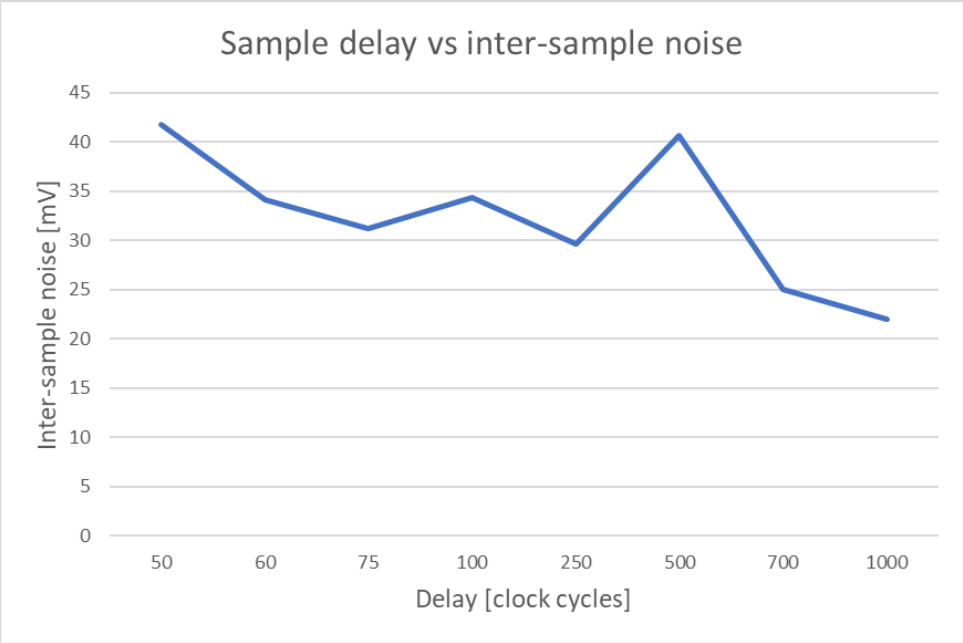

Fig. 4: Inter-sample noise – sampling delay dependency

The first tests were done with a small analogue filter capacitor (C = 151pF), to allow most noise frequencies to pass through the filter and into the converter. After choosing the sampling delay, we have replaced the capacitor with a larger one (C = 1nF) and noted the differences (Fig. 5). Although the mean performance is better, increasing the capacitance will only enlarge the capacitor and increase the group delay introduced by it.

The next parameter we analyzed was the dependence between the frequency of the analog switch address and the inter-sample noise. The implemented algorithm allows the user to set the analog switch address frequency for the DG408DJs. We have analyzed three frequencies: 119.5Hz, 239.02Hz and 478.94Hz to see each of their performance.

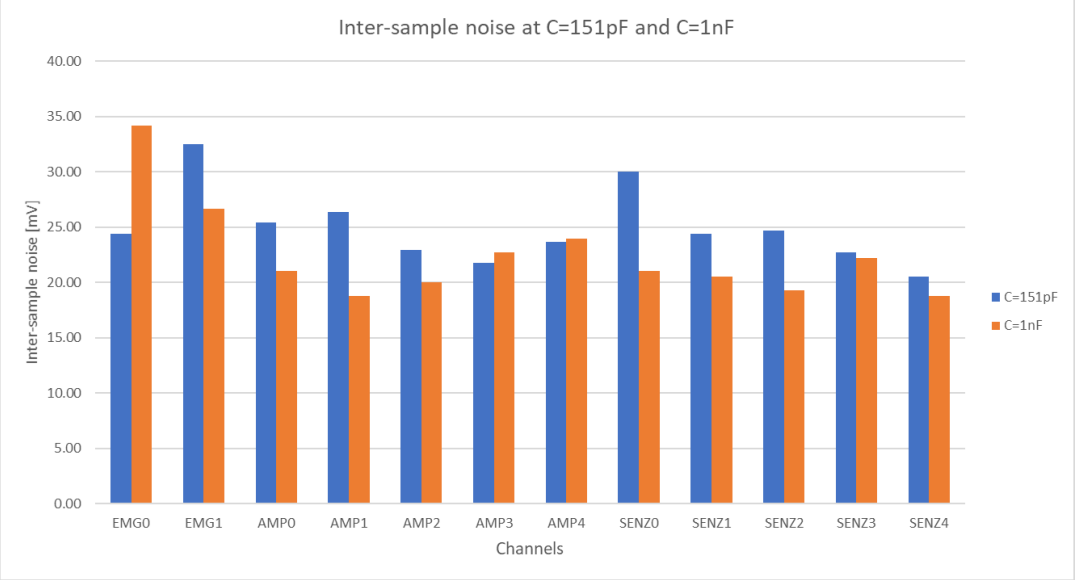

Fig. 5: Inter-sample noise at different filter capacitance levels

An important observation can be made regarding the channels with higher voltage levels (EMG1, SENZ3): they have significantly higher noise peak to peak voltage than those connected to ground (EMG0, SENZ1, SENZ2).

4. Conclusions

The proposed system has performed well, in spite of its reduced complexity. The interface can be miniaturized by using SMDs instead of THTs, but the XC7A35TCPG236-1 FPGA is a compact and well-suited solution, which contains all the devices needed for the data processing block (DSPs, integrated analogue to digital-converter).

The proposed circuit contains low-power integrated components and can work for a prolonged period of time, which is a perfect fit for a prothesis application. Furthermore, using the XADC integrated in the FPGA matrix greatly increases the spatial efficiency of the system and lowers both the delay and the traces that would have been needed if we were to use an external converter. Even considering all the limitations imposed by the XADC, such as low impedance voltage sources, stables voltages between 0 and 1V and communication protocol between the XADC and the FPGA using the DRP, the XADC is still worth using in a control system for an exoprosthesis.

The integrated DSPs increase the computational power of the FPGA, allowing more efficient implementations for computing-heavy algorithms, such as FIR filters and dynamic PWM generators.

The usage of ampere meters in the system is a great method for both monitoring the motors and limiting the power consumption of the whole system. Although a rotary encoder would offer better positional information, choosing the ampere meter solution frees up space in the mechatronic structure of the prosthetic hand. Furthermore, limiting the current draw of the motors increases their life expectancy and offers an extra safety mechanism for the sensorial interface.

In conclusion, the system, despite its simplicity, is quite robust and easy to use. It can be further improved by including higher order analog filters and shorter analog traces (to decrease the attenuation and increase the noise resilience). The true advantage of this system is its spatial efficiency, one of the most important aspects in the prosthesis control system. In the next stage, we will use the system mentioned in this paper on a real patient.

Acknowledgement

The authors gratefully acknowledge the support provided by the NerveRepack project, which is co-funded by the European Union under Grant Agreement No. 101112347. The continuous guidance and resources provided by the project were instrumental in achieving the objectives of this study.

R E F E R E N C E S

1. *Yuan B, Hu D, Gu S, Xiao S, Song F.* The global burden of traumatic amputation in 204 countries and territories. Front Public Health. 2023; Vol. **11**, Iss:1258853, Published on 2023 Oct 20. doi:10.3389/fpubh.2023.1258853
2. *Morand, R., Brusa, T., Schnüriger, N., Catanzaro, S., Berli, M., & Koch, V. M.* FeetBack-Redirecting touch sensation from a prosthetic hand to the human foot. Frontiers in neuroscience, Vol. **16**, 1019880. https://doi.org/10.3389/fnins.2022.1019880, 2022
3. *Roche AD, Bailey ZK, Gonzalez M, et al.* Upper limb prostheses: bridging the sensory gap. J Hand Surg Eur Vol. 2023, Vol. **48**, Iss. 3, pp.182-190. doi:10.1177/17531934221131756
4. *Song, H., Hsieh, TH., Yeon, S.H. et al.* Continuous neural control of a bionic limb restores biomimetic gait after amputation. Nat Med 30, 2010–2019, 2024. https://doi.org/10.1038/s41591-024-02994-9
5. *Biddiss EA, Chau TT.* Upper limb prosthesis use and abandonment: a survey of the last 25 years. Prosthet Orthot Int. 2007 Sep; Vol.**31** Iss.:3, pp:236-57. doi: 10.1080/03093640600994581. PMID: 17979010.
6. *Ionescu, O.N.; Franti, E.; Carbunaru, V.; Moldovan, C.; Dinulescu, S.; Ion, M.; Dragomir, D.C.; Mihailescu, C.M.; Lascar, I.; Oproiu, A.M.; et al.* System of Implantable Electrodes for Neural Signal Acquisition and Stimulation for Wirelessly Connected Forearm Prosthesis. Biosensors 2024, Vol.**14**, Iss.31, WOS:001149201300001
7. Spart-3 FPGA datasheet– https://docs.amd.com/v/u/en-US/ds099
8. JLCPCB – https://jlcpcb.com/